Preliminary design of a mechanically pumped cooling system for active antennae

Henk Jan van Gerner[1], T.H. van den Berg, and Johannes van Es
NLR – Royal Netherlands Aerospace Centre, Amsterdam, The Netherlands

Anne Tailliez[2], Andrew Walker
AIRBUS Defence and Space, 31400 Toulouse, France

Cristina Ortega[3], Monica Iriarte Centeno, and Charlton Castro
AVS – Added Value Solutions, 20870 Elgoibar, Spain

The satellite telecommunications industry is currently undergoing significant evolutions. Future communication satellites need to accommodate a rapidly growing demand in data transfer, combined with more flexibility. For example, there is a strong need for Very High Throughput Satellites capable of delivering up to Tb/s over wide coverage areas and an active phased array antenna is a powerful enabler to achieve that. However, cooling of active antennas requires the use of a highly efficient thermal control system because it has many heat sources (hundred or more), high local heat fluxes (20W/cm² at evaporator interface), high overall dissipation (around 10 kW), and isothermal requirements on the amplifier chain. These conditions are very difficult to solve with current thermal control solutions (e.g. heat pipes or loop heat pipes), but require a two-phase mechanically pumped fluid loop (MPL). In a MPL, a pump circulates a fluid which evaporates when it absorbs the waste heat from the active antenna. In the EU funded IMPACTA project, a demonstrator for such a MPL is being designed and built. This paper describes the preliminary design for this demonstrator, including the fluid selection and tests on evaporator samples.

Nomenclature

ρ	=	Fluid density (kg/m^3)
μ	=	Dynamic viscosity (N/m^2 s or kg/(ms))
σ	=	Surface tension (N/m)
d	=	Inner diameter tube (m)
f	=	Friction factor (-)
h_{lv}	=	Specific latent heat of vaporization (J/kg)
L	=	Length of tube (m)
$\dot{m}$	=	Mass flow (kg/s)
P	=	heat input (W)
p	=	pressure (N/m^2)
Re	=	Reynold number (-)
Q	=	Volume flow (m^3/s)
T	=	Temperature (°C)
v	=	Fluid velocity (m/s)

I. Introduction

In the IMPACTA project, which is led by AVS, a demonstrator of a two-phase mechanically pumped fluid loop (MPL) for an active antenna for a communication satellite is being developed. This paper focuses mainly on the

[1] R&D Engineer, Thermal control systems, Henk.Jan.van.Gerner@nlr.nl, +31 88 511 4628.
[2] Product User, Thermal and Mechanical Products, Anne.Tailliez@airbus.com, +33 56 219 5377
[3] Head of Space Area, space@a-v-s.es, +34 943 821 841

preliminary system analysis for the fluid selection of the mechanically pumped fluid loop, and the preliminary evaporator design and tests on evaporator samples. Figure 1 shows a schematic drawing of a mechanically pumped fluid loop. A pump transports liquid to an evaporator that is mounted on e.g. an active antenna. In the evaporator, the heat from the active antenna is absorbed and the liquid (partly) turns into vapour. The vapour/liquid mixture then flows to the radiator/condenser. In the radiator, the absorbed heat from the active antenna is radiated into space, and the vapour is turned back into liquid. The pressure and temperature of a two-phase fluid are coupled. As a result, the temperature of the liquid/vapour mixture is the same in the entire system (assuming a negligible pressure drop), and independent of the heat input or heat sink temperature. The accumulator controls the saturation temperature in the system. Two-phase mechanically pumped loops have several advantages compared to other thermal control systems, such Heat Pipes (HP), Loop Heat Pipes (LHP) or single-phase liquid MPL[1]:

- The fluid saturation temperature (which is set by the accumulator) is independent of the heat load or heat sink temperature. This results in a uniform temperature of the active antenna.
- The tubing diameter can be much smaller than for a single-phase liquid MPL, LHP or HP. This tubing can easily be routed along all the heat sources.
- The two-phase heat transfer coefficient is very high compared to single-phase MPL, HP, or LHP. This high heat transfer coefficient results in a smaller temperature difference between the fluid and the active antenna. As a result, a higher fluid temperature can be used, which results in a smaller radiator surface.

A drawback of a pumped two-phase system is that it requires a mechanical pump. Furthermore, the design of a two-phase system is more complex than the design of a single-phase system or a system with heat pipes. As a result, the TRL of this technology is relatively low and is not often used for space applications, despite the enormous advantages that this technology provides. As far as the authors know, there is only one two-phase MPL that is operating in space; which is the tracker thermal control system of the Alpha Magnetic Spectrometer (AMS-02) on ISS[2].

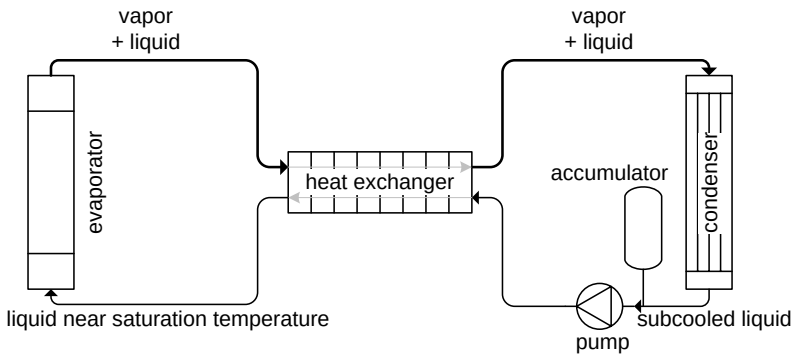

Figure 1 Schematic drawing of a two-phase pumped loop with recuperator (also called heat exchanger). The recuperator warms the subcooled liquid leaving the condenser to saturation temperature.

II. Fluid Preselection

The selection of a suitable fluid is one of the first and most important steps for the design of a thermal control system. However, the number of fluids to choose from is very large. For example, the NIST Reference Fluid Thermodynamic and Transport Properties Database REFPROP[3] contains around 149 different fluids. Since the fluid properties vary with temperature, a fluid that functions very well at a certain temperature may not be suitable at another temperature. For this project, a systematic fluid selection approach has been used. First a preselection of fluids is made with the NLR Fluid Selection Tool[4]. These fluids are analyzed in more detail with the NLR Cooling System Analysis Tool[5], after which a final fluid is selected. This is described in the next sections.

A. Figure of Merit

For a two-phase thermal control system, it is important that the tubing has a small diameter. Not only is the routing of the tubing much simpler when the diameter is small, but the system volume also scales with the square of the diameter, and a higher system volume results in larger and heavier components. For this reason, it is important to minimize the diameter of the tubing. However, a small diameter of the tubing results in a large pressure drop. This pressure drop is not only disadvantageous for the pump, but large pressure gradients in a two-phase cooling system also results in large temperature gradients (since pressure and temperature are related in a two-phase cooling system).

For this reason, an important characteristic of the fluid for two-phase thermal control system is a small pressure drop for a certain heat transport and geometry.

The pressure drop in the liquid tubes can be calculated with the Darcy-Weisbach equation[6]:

$$\Delta p_l = f_l \frac{L}{d} \frac{\rho_l v_l^2}{2} \text{ with } v_l = \frac{\dot{m}}{\rho_l \pi d^2 / 4} \text{ and } \dot{m} = \frac{P}{h_{lv}} \quad \textbf{(1)}$$

The flow in the tubes is turbulent, and the friction factor can be approximated with the Blasius correlation for turbulent flow in smooth-walled tubes[6]:

$$f_l = \frac{0.3164}{\mathrm{Re}_l^{0.25}} \quad \textbf{(2)}$$

The same equations can be used for the vapour tubes, when the subscript *l* is replaced by *v*. In order to find a fluid with a small pressure drop, Eq. (1) and Eq. (2) are rearranged to (assuming that half of the fluid is liquid and half is vapour):

$$\Delta p \propto \overbrace{\left(\frac{\mu_l^{1/4}}{\rho_l h_{lv}^{\ 7/4}} + \frac{\mu_v^{1/4}}{\rho_v h_{lv}^{\ 7/4}} \right)}^{\text{fluid dependent}} \overbrace{\frac{L}{d^{19/4}}}^{\text{geometry dependent}} \overbrace{P^{7/4}}^{\text{Heat input}} \quad \textbf{(3)}$$

The equation for the pressure gradient in the system is rearranged in a fluid dependent part, a geometry dependent part (i.e. the length and diameter of a tube) and the heat input. The inverse of the fluid dependent part in the equation above can be used to find a fluid that results in a small pressure gradient. This inverse is called a Figure of Merit, which should be as high as possible:

$$M_{\text{low } \Delta p} = \frac{1}{(\mu_l^{1/4} / (\rho_l h_{lv}^{\ 7/4}) + \mu_v^{1/4} / (\rho_v h_{lv}^{\ 7/4}))} \quad \textit{Figure of Merit based on low pressure gradient} \quad \textbf{(4)}$$

In the Fluid Selection Tool, the safety of a fluid is rated with the NFPA 704 standard[13] in the form of a 'safety diamond' (see Figure 2 for the NFPA diamond of ammonia). This NFPA rating is divided in four categories which are color-coded with red indicating flammability, blue indicating level of health hazard, yellow for chemical instability, and white containing codes for special hazards. Each of health, flammability and instability is rated on a scale from 0 (minimal hazard) to 4 (severe hazard). In this project, it is required that the NFPA rating of the fluid (in any category) is 3 or lower.

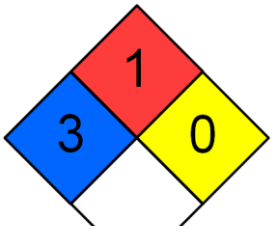

Figure 2 NFPA diamond for ammonia

Figure 3 shows the Figure of Merit M for all fluids in the REFPROP[3] fluids database with a NFPA rating of 3 or lower, excluding the fluids that are banned according to the Montreal protocol. On the horizontal axis, the saturation temperature of the fluid is shown. The fluid saturation temperature of the IMPACTA application is around 80°C. Future applications could operate at a fluid temperature up to 100°C. These temperatures are indicated with the dashed grey vertical lines. For clarity reasons, the labels of some fluids with a low Figure of Merit are not shown in Figure 3. The Figure of Merit for ammonia is much higher than for any other fluid (e.g. an order of magnitude larger than for R134a). This means that the tubing diameter for a system with ammonia will be much smaller than for other fluids. Fluids with a NFPA rating of 4 (e.g. propyne, R40 or DME) are not shown in the figure, but all these fluids also have a much lower Figure of Merit than ammonia. Ammonia is commonly used in (industrial) cooling applications, but because of its toxicity (ammonia has a NFPA rating of 3 for health) and issues with material compatibility, it is more difficult to use than other fluids. There

are many fluids with a much lower Figure of Merit than ammonia, but with a more favorable NFPA rating (i.e. a NFPA rating of 2 or lower). These are shown in Figure 4.

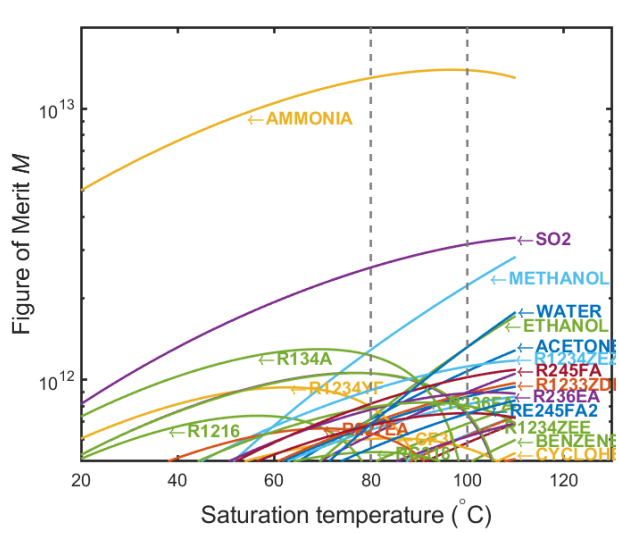

Figure 3 Figure of Merit for all fluids in the REFPROP database with a NFPA rating of 3 or lower

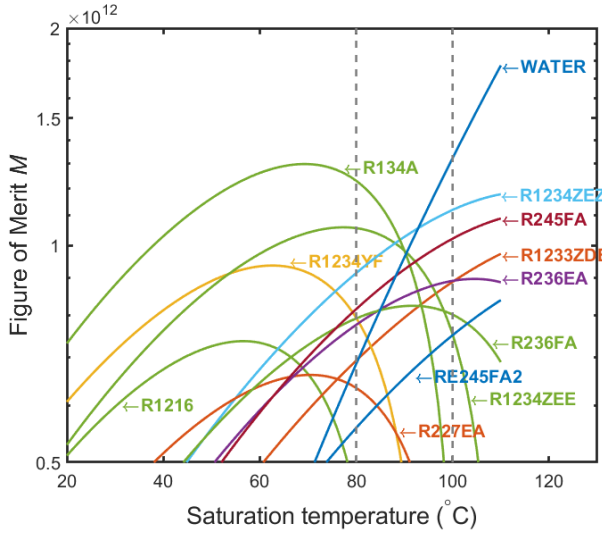

Figure 4 Figure of Merit for all fluids in the REFPROP database with a NFPA rating of 2 or lower

B. Pre-selected fluids

Table 1 shows the fluid properties for ammonia (which has a NFPA rating of 3), and the fluids with the highest Figure of Merit in NFPA category 0, 1 and 2. Besides fluid properties, this table also shows some system characteristics that are calculated by the Fluid Selection Tool, namely the required volume flow and the required tube diameter. From the Figures of Merit, it can be seen that ammonia has about 16 times higher Figure of Merit than e.g. R245fa. This means that a system with ammonia would have a 16 times lower pressure drop than the same system that is filled with R245fa. Normally, a system with ammonia will have a smaller diameter tubing. The typical tubing diameter for a two-phase transport tube is calculated by the Fluid Selection Tool in order to get a rough indication of the tubing diameter. In this calculation, it is assumed that the length of the tube is 12 meter, the mass flow corresponds to 10 kW heat input, the vapour mass fraction is 0.7 and the accepted pressure drop is 0.20 bar. The pressure drop is calculated with the Friedel two-phase pressure drop correlation[7]. As can be seen from the table, the tube inner diameter with ammonia has to be 9.7 mm, while with R245fa it has to be 17.6 mm in order to obtain a similar pressure drop in a system.

For briefness, some fluids from Figure 4 are excluded from table 1. For example, R1234ze(Z) and R245fa have a very similar performance (R1234ze(Z) has actually been developed as a replacement for R245fa). However, a very large drawback of R1234ze(Z) is that its freezing temperature of -35°C is much higher than that of R245fa. R236ea also has a high freezing temperature. Because of the high freezing temperatures of R1234ze(Z) and R236ea (and because they don't have a performance that is much better than other fluids), these fluids are not included in table 1. The fluids in this table are analyzed in more detail with the System Analysis Tool. This is described in the next section.

Table 1 Relevant properties at 80°C for fluids with the highest Figure of Merit.

Fluid	pressure (bar)	Triple point (°C)	heat of evaporation h_{lv} (kJ/kg)	Surface tension σ (mN/m)	Required volume flow (lph)	Typical tube inner diameter (mm)
Ammonia	41	-78	875	8.66	116	9.7
R1234ze(E)	20	-104	110	2.31	499	16.5
R245fa	8	-103	154	6.89	286	17.6
R236fa	12	-93	106	3.55	427	17.7
R1233zd(E)	7	-78	158	7.8	292	18.1

III. System Analysis for Fluid Selection

A. Steady-state analysis with the Cooling System Analysis Tool

To make a trade-off between the pre-selected working fluids, detailed steady-state simulations have been made with the Cooling System Analysis Tool[5]. This software numerically solves (in MATLAB) the steady-state mass and enthalpy equations for a two-phase fluid. The frictional pressure drop in the system is calculated with the Darcy–Weisbach equation in which the friction factor for turbulent flow is calculated with the Colebrook equation, and the friction factor for laminar flow is calculated with 64/Re. For two-phase flow, the pressure drop is calculated with the Friedel correlation[7]. The heat transfer coefficient is calculated with the Gnielinski correlation[6] for turbulent liquid flow, with the Gungor-Winterton correlation for evaporating flow[8], and with the Shah correlation for condensing flow[9]. The fluids in Table 1 have been analyzed with the simulation tool and the results for ammonia and R245fa are described in more detail in the next sections. From these calculations, the volume and mass of the system component can be estimated.

B. Simulation results for ammonia

Figure 5 shows the calculated temperatures in the system, together with calculated system parameters. In this simulation, there are 100 heat sources with a heat dissipation of 100W each (so 10 kW in total) divided over 10 parallel evaporator branches. The input parameters for the model are indicated with red text, while the output is in black text. The mass flow is chosen such that 70% of the liquid is evaporated in the evaporator. The typical tubing inner diameter from Table 1 is used for the two-phase tubing, while the diameter of the liquid tubing is 0.6 times this value. The dimensions of all other components (condenser, evaporators, etc.) are also scaled with the typical tubing diameter. The System Analysis Tool calculates the mass of different components and includes the wick material that is used inside the accumulator in order to control the location of the liquid. Figure 6 shows the calculated vapour mass fraction in the system, while Figure 7 shows the calculated pressure. The pressure difference of 0.92 bar will be higher in an actual system. However, the calculation model does not yet contain items like bends, manifolds, and particle filters, so the actual pressure drop will be larger than what is currently calculated. This will be addressed in the detailed design of the system.

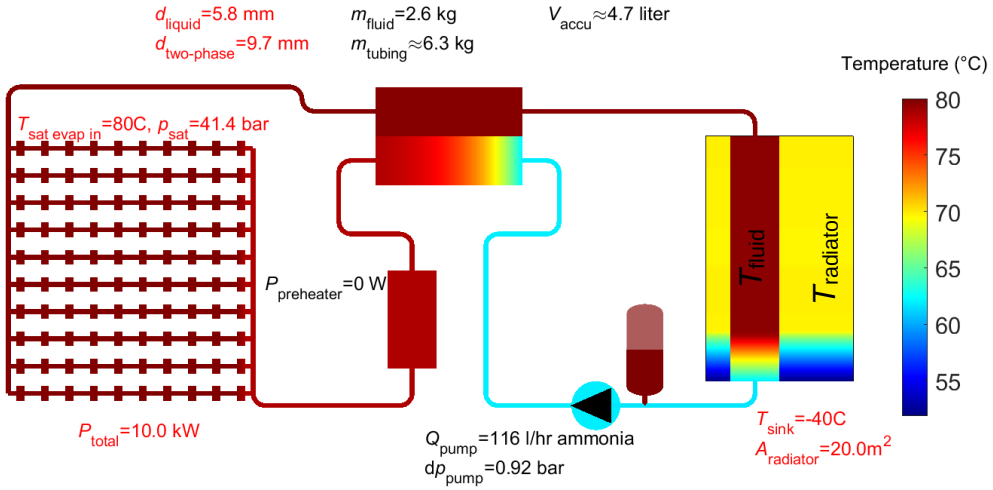

Figure 5 Calculated temperature for a MPL with ammonia

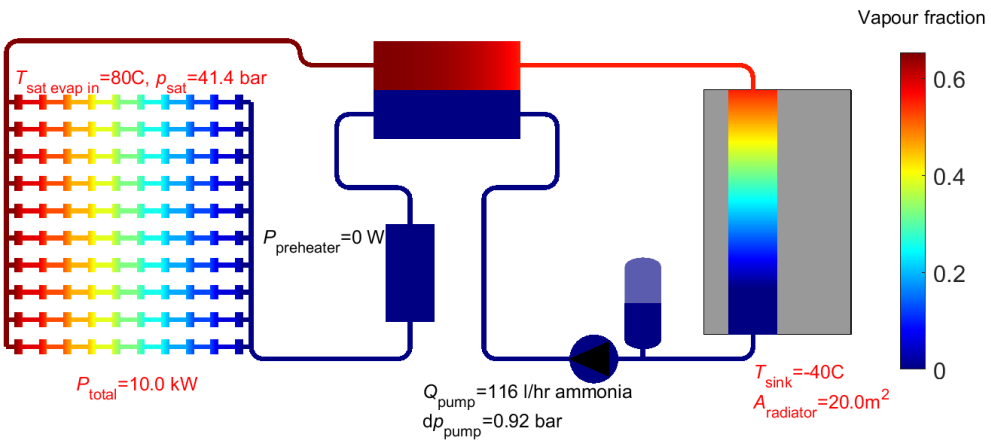

Figure 6 Calculated vapour mass fraction for a MPL with ammonia

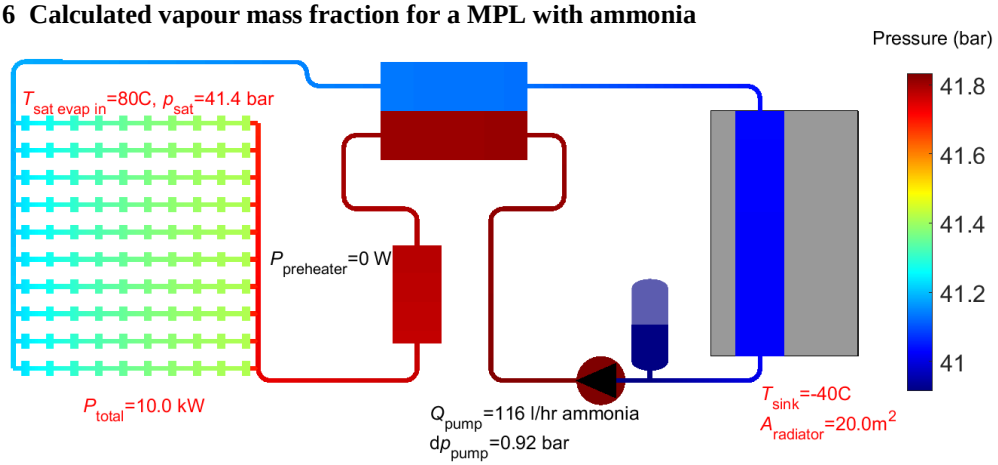

Figure 7 Calculated pressure for a MPL with ammonia

C. Simulation results for R245fa

In this section, the results for R245fa are presented. Only the figure with the calculated temperatures is shown, since the figures for vapour mass fraction and pressure are very similar to that of ammonia. Figure 8 shows the calculated temperatures for R245fa. The accumulator volume is approximately 15 liter, compared to the 5 liters needed for ammonia. The calculated mass of the vessel is similar as for ammonia, because of the lower saturation pressure of R245fa. The required volume flow of 286 l/hr for R245fa is 2.5 times larger than for ammonia. The pressure difference over the pump is similar, because the diameter of the tubing is chosen such that these pressure differences are similar (see Table 1). The heat transfer coefficient in heat exchangers is smaller for R245fa than for ammonia. This results in a larger required radiator area for R245fa. Also, the recuperator is less efficient because of the lower heat transfer coefficient and as a result, electrical preheater power is required to raise the liquid temperature to the desired value before it enters the evaporator. Instead of using electrical preheater power, a larger recuperator could also be used.

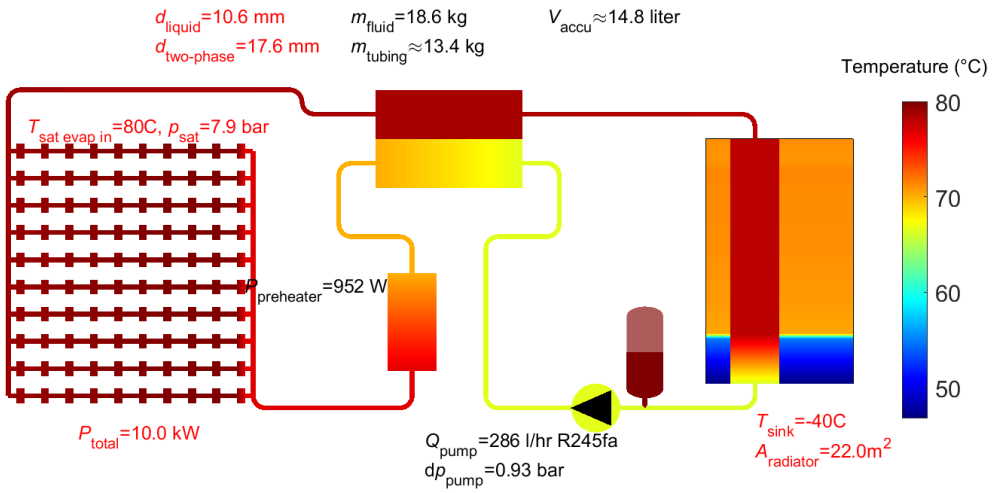

Figure 8 Calculated temperature for a MPL with R245fa

IV. Fluid Stability, Material Compatibility, and Future Availability

In a space application, the fluid in the system is exposed to ionizing radiation. This ionizing radiation consists mainly of highly energetic protons and helium nuclei. Due to the exposure of the fluid to radiation, chemical bonds are broken and other substances (such a H_2) will form. These substances could damage the system, for example gas bubbles could block small fluid channels or cause vibrations in the pump. Ammonia is extensively used in heat pipes and loop heat pipes and the amount of substances formed due to radiation is well known[10]. No issues are foreseen with the radiation stability of ammonia. A gas trap is included in the system that will capture small amounts of gas that are formed. Despite extensive research, no information on the radiolysis of other fluids could be found. The radiation stability of these fluids is therefore unknown.

Ammonia has an excellent compatibility with stainless steel 316. Ammonia also has a good compatibility with most aluminium alloys, although aluminum alloys with a higher copper content are more susceptible to corrosion. Corrosion might also occur when combinations of stainless steel and aluminum are used. All other fluids in Table 1 have an excellent compatibility with aluminium, stainless steel and titanium.

R236fa and R245fa in Table 1 are hydrofluorocarbons (HFCs) that were developed to replace ChloroFluoroCarbons (CFCs) and HydroChloroFluoroCarbons (HCFCs) that damage the ozone layer. CFCs and HCFCs are banned according to the Montreal protocol. R236fa and R245fa don't damage the ozone layer and are (almost) non-flammable, but they have a high global warming potential (more than 150 times larger than carbon dioxide). EU regulations (e.g. the MAC directive), prohibits the use of fluorinated gases with a global warming potential of more than 150 times greater than carbon dioxide in all new cars and vans produced from 2017. In all other applications, the HFCs fluids are being phased-out when alternatives are available. This could mean that availability of these fluids (R236fa and R245fa) in the far future could be an issue.

R1234ze(E) and R1233zd(E) are HydroFluoroOlefins (HFOs) that have been developed as replacement for the HFCs. These fluids have a low global warming potential. However, these fluids are relatively new, and it might be too early to tell whether these fluids represent the long term solution or not. For example, the German Environment Agency calls for a ban[11] of R1233zd, since it has a non-negligible ozone depletion potential of 0.00034.

Ammonia (also known as refrigerant R717) is used on a wide scale in industrial refrigeration, but also in many other applications. No issues with its availability in the future are foreseen.

V. Final Fluid Selection

Table 2 shows the summary of the analysis results. The mass of the system consist of two complete systems; a primary and redundant system. Each system has a primary and a redundant pump (so there are 2 pumps per system, 4 in total). The mass of the radiator is included in the total mass. In the mass calculation, the amount of required wick material inside the accumulator is included and this calculation shows that R1234ze(E) is not possible because it has a too low surface tension. Ammonia has the highest NFPA rating due to its toxicity. This means that it is more difficult to work with and more safety measures have to be taken. Ammonia is compatible with stainless steel and aluminum

but some caution is required. Despite these drawbacks, ammonia is selected as the fluid for IMPACTA. The volume flow of ammonia is at least two times lower than that of other fluids. The mass is more than 100 kg lower, and the system volume is around 3 times lower. Furthermore, ammonia is the only fluid with known good radiation stability and the only fluid for which it is sure that future availability will not be an issue.

Table 2 Summary of results for different fluids

Fluid	NFPA	Volume flow (lph)	Total system mass (kg)	Accumulator volume (liter)	Radiation stability	Long term availability	Compatibility
Ammonia	3	114	162	4.7	Good	Good	Corrosion can occur
R1234ze(E)	2	489	Not possible	14.0	Unknown	Probably good	Good
R245fa	2	280	301.2	14.8	Unknown	Could be an issue	Good
R236fa	1	418	372	15.6	Unknown	Could be an issue	Good
R1233zd(E)	2	286	280.6	15.5	Unknown	Probably good	Good

VI. Preliminary Evaporator Design

A. Background

In a thermal control system, the size of the radiator has a very large influence on the total system mass. Since the required radiator surface area (approximately) scales with T_{fluid}^{-4}, it is of the utmost importance to use an as high as possible fluid temperature. The largest temperature gradients in the cooling system usually occur between the heat source and the fluid. A thermally efficient evaporator is therefore very important in minimizing the total mass of the cooling system. In the IMPACTA project, several evaporator designs will be made. The NLR will make an evaporator design with 'conventional' geometry (straight channels, no advanced surface structures) and this evaporator is described in the next section. The evaporator performance might be improved by using novel techniques and this is studied by other partners in the consortium. For example, CEA studies the effect of surface treatments and advanced channel geometries (instead of simple straight channels) are studied by Diabatix. Furthermore, it might be possible to integrate the evaporator close to the heat sources, instead of mounting an evaporator onto an electronics box. This is studied by CERN.

B. Evaporator layout

In the IMPACTA project, the evaporator will be made from aluminium Multi Port Extrusions (MPE). These are flat extruded aluminum profiles with internal channels. Figure 10 shows a photo of a cross section of a MPE. Two strips of MPE will be attached to a row of antenna heat sources. The strip closest to the heat source is the primary evaporator, while the MPE strip on top of the primary evaporator is the redundant evaporator. At the inlet of each strip is an inlet manifold that distributes the liquid over the parallel channels of the MPE and at the MPE outlet is an outlet manifold. Each inlet manifold is connected to a liquid tube that distributes the liquid over the parallel branches. Figure 9 shows a CAD drawing of the preliminary design of the MPE evaporators. Tests have been carried out with MPE samples to test the performance of the MPE evaporators. These tests are described in the next section.

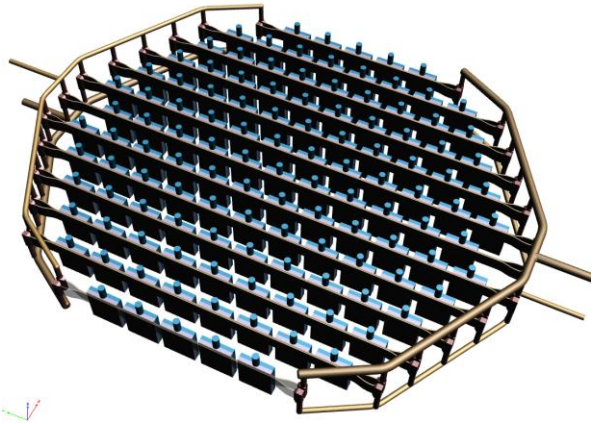

Figure 9 CAD drawing of the preliminary design of the MPE evaporators

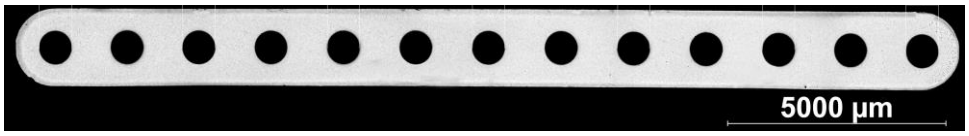

Figure 10 Photo of a cross-section of an aluminium Multi Port Extrusions

VII. Evaporator Sample tests

A. Evaporator Sample

Figure 11 shows a CAD drawing of a MPE evaporator sample. The evaporator sample consists of a MPE profile with a length of 25 cm that is inserted at both ends into inlet and outlet manifolds. The inlet manifold distributes the liquid over the 13 parallel channels. A 100W copper heater block with two 12 mm x 12 mm hotspots is used to simulate the heat load of one antenna unit. This copper heater block is clamped to a 6 mm thick aluminium plate that represents the housing of an antenna unit. The MPE profile is clamped against this aluminum plate. There will be two evaporators attached to a single antenna unit; the primary evaporator and the redundant evaporator. These evaporators are located on top of each other. When the primary system fails, because e.g. it is punctured by a micro-meteoroid, the redundant evaporator has to cool the system. In the test setup, this 'punctured' primary evaporator is represented by an 'empty' MPE profile that is clamped between the 'filled' MPE profile and heat source. This configuration is called MPE1. The MPE2 configuration has the filled MPE profile between the empty MPE profile and the heat source. The copper heater block and the aluminium plate have several holes with a diameter of 0.6 mm. Figure 12 shows a cross-section of the MPE1 evaporator which shows the location of the these holes. Temperature sensors with a diameter of 0.5 mm are inserted into the holes, such that the temperature is measured beneath the center of the hotspots.

In an active antenna, there are around 10 antenna units on a single branch. Liquid near saturation temperature enters the MPE profile of each branch. The vapour mass fraction of the fluid is increased at each antenna unit, until it has a vapour mass fraction of around 0.7 at the exit of the last antenna unit on a branch. In the test setup, only one active antenna unit is simulated. The heat load of the 0 to 9 active antenna units that can be located before this simulated active antenna unit is represented by a pre-evaporator. This pre-evaporator has a maximum power of 900 W and can therefore simulate the heat load of 0 to 9 antenna units. The vapour mass fraction that enters the simulated active antenna unit can be set by this pre-evaporator.

Figure 13 shows a photo of the NLR two-phase test facility[12] with the evaporator samples MPE1 and MPE2 installed in a parallel configuration.

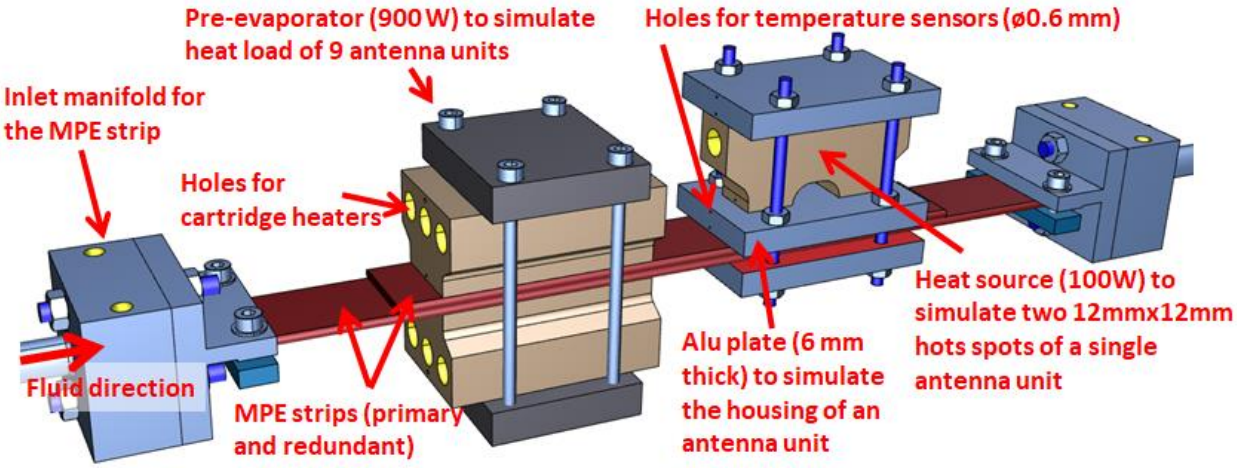

Figure 11 CAD drawing of the MPE1 evaporator sample

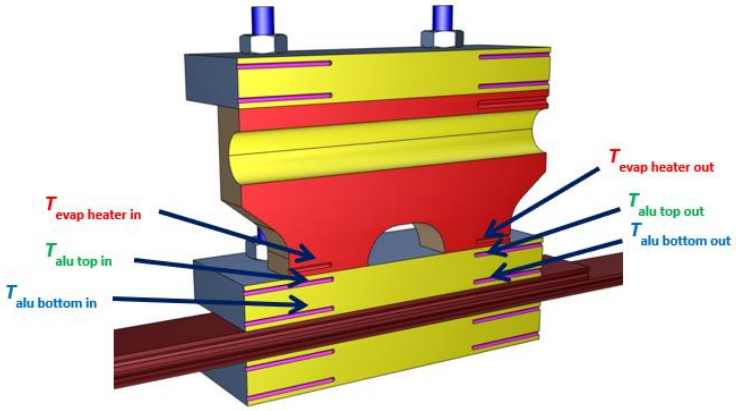

Figure 12 Cross-section of the MPE1 evaporator sample with the locations of the temperature sensors

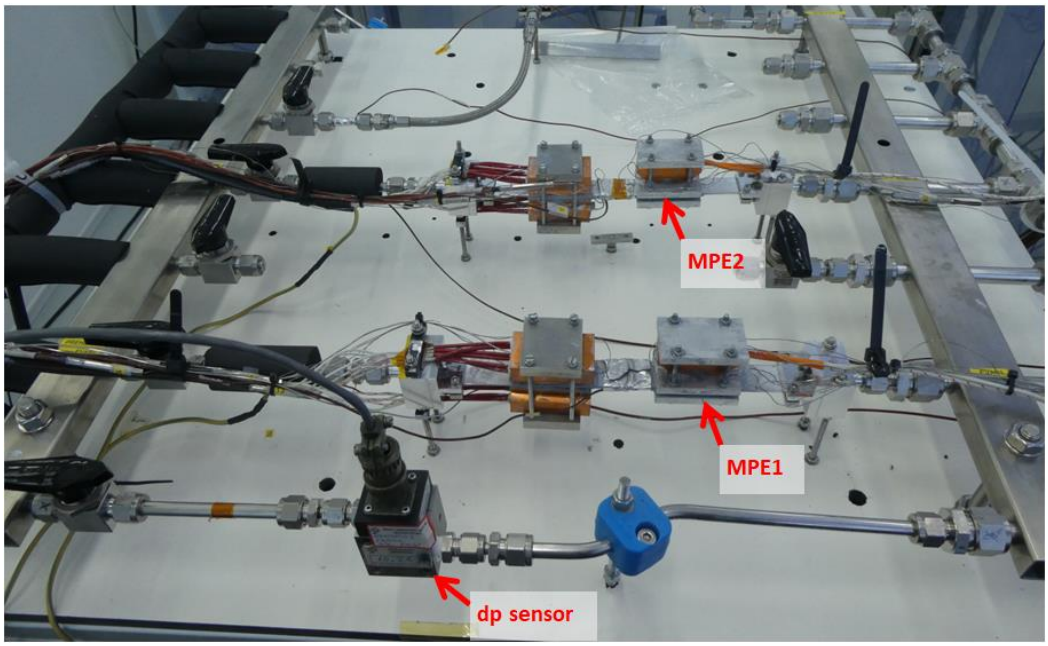

Figure 13 Photo of the NLR Two-Phase Test Facility with 3 evaporator samples MPE1 and MPE2 installed in a parallel configuration. The thermal insulation around the test samples was removed for taking the photo

B. Test results

The ammonia massflow is set to 3.2 g/s. The valves of the MPE1 and MPE2 branch are both opened, and each branch should receive approximately 1.6 g/s. Figure 14 shows the heater power that is applied during the measurement. The solid lines indicate the heater powers for the MPE1 branch, while the dashed lines indicate the heater powers for the MPE2 branch. The MPE power is first set to 100W (which is the requirement). Around *t*=6.3 hours, the MPE power is set to 200W to see if a higher heat load is also possible. The pre-evaporator power is increased in steps. The powers to branch 1 and 2 are usually set to the same value, except around t=5.5 hours. Around this time, the MPE1 and pre-evaporator power of branch 1 (which are indicated with solid lines in Figure 14) were reduced. This was done to see if the two parallel branches are able to manage an imbalance in the heat load. Figure 15 shows the vapour mass fraction at the inlet and outlet of the MPE evaporator samples. The vapour mass fraction of MPE1 is indicated with a solid line, while the vapour mass fraction of MPE2 is indicated with a dashed line. The vapour mass fraction is not directly measured, but derived from the heat input and the massflow (an equal massflow through both branches is assumed). The solid and the dashed lines (indicating branch 1 and 2) are on top of each other, except between 5.5 and 5.8 hours, where the heater power to branch 1 was reduced. As a result, the vapour fraction in and out of MPE1 becomes zero during this time (i.e. the flow is in the liquid phase).

Figure 16 shows the measured temperatures in MPE1 while Figure 17 shows the measured temperatures in MPE2. The exact location of the temperature sensors is indicated in Figure 12. The solid colored lines indicate the temperatures at the inlet of the evaporator while the colored dashed lines indicate the temperatures at the outlet of the evaporator. The black line indicates the saturation temperature (which is derived from the pressure sensor). At the start of the measurement, all measured temperatures are just (approximately 2°C) below the saturation temperature of 80°C. When the MPE power is set to 100W, the temperature in the copper heat block ($T_{\text{evap heater in/out}}$) quickly rise to 98°C in MPE1 and 96°C in MPE2. The temperature in MPE1 is slightly higher than in MPE2 because MPE1 has the empty MPE profile between the heat source and the filled MPE profile. The vapour mass fraction at the inlet of the MPE is increased in steps from 0 to 0.6 by increasing the pre-evaporator power. The measured temperatures are nearly independent of the vapour mass fraction at the inlet of the evaporator. When the heater power to MPE1 is set to zero around t=5.5 hours, the temperatures quickly drop to just below the saturation temperature. There is no influence on the temperatures in MPE2. This shows that the parallel branches are able to handle an uneven heat load. When the heat load on the MPE is increased to 200W (which is twice the requirement), the temperatures increase. However, there is no indication of dry-out. This means that the MPE can cool a much higher heat load than is required, and that there is therefore sufficient margin in the evaporator design of the system.

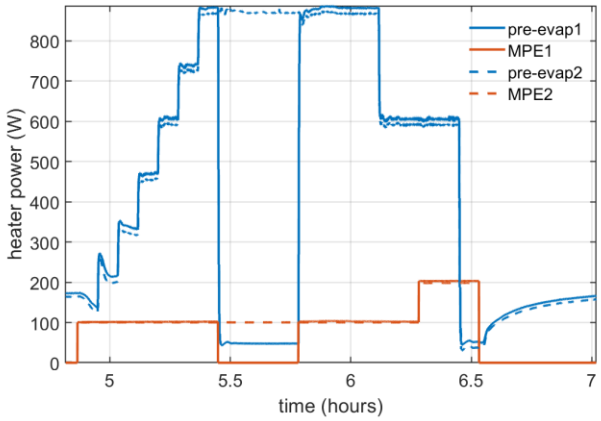

Figure 14 Heater powers applied during the test for branch 1 (solid lines) and branch 2 (dashed lines)

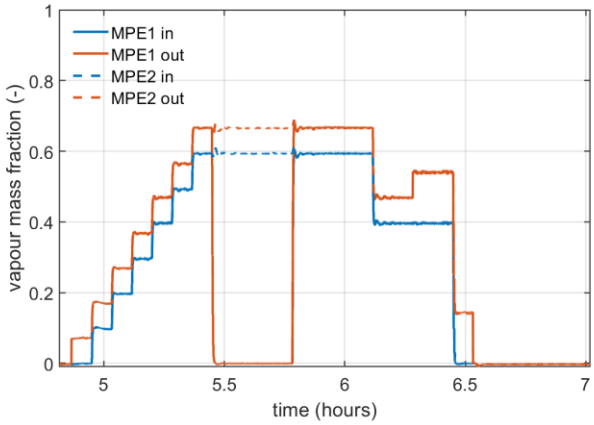

Figure 15 Vapour mass fraction at inlet and outlet of MPE1 (solid lines) and MPE2 (dashed lines)

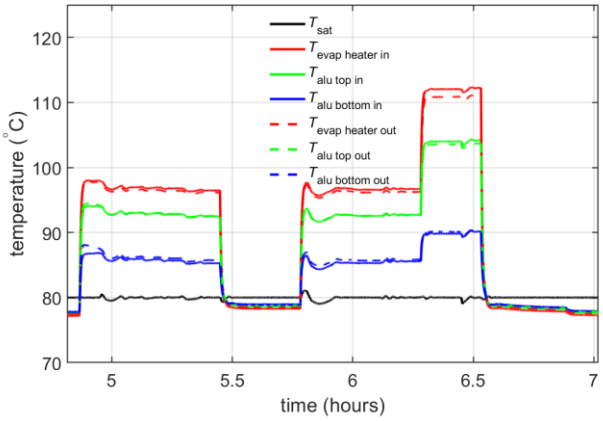

Figure 16 Measured temperatures in MPE1

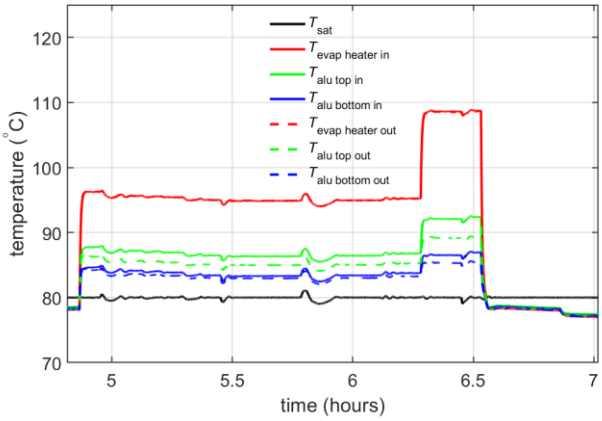

Figure 17 Measured temperatures in MPE2

VIII. Conclusion

This paper discusses the preliminary design of a two-phase MPL for an active antenna for a communication satellite. The fluid selection was used to compare the system mass and volume for different fluids, such that a good trade-off has been made between the fluids. Ammonia is selected as the working fluid for this system, because a

system with ammonia will have a much smaller mass and volume than a system with another fluid. The paper also discusses the preliminary design of the evaporator. Measurements on evaporator samples were carried out to test the feasibility of this preliminary design. These tests show that the evaporator samples have an excellent performance. The results in this paper will be used to make the detailed design of the system and the evaporators.

Acknowledgments

This project is carried out in close cooperation with Added Value Solutions (AVS), Airbus Defence and Space, CEA, CERN, and Diabatix. This project has received funding from the European Union's Horizon 2020 research and innovation programme under grant agreement No 822027.

This publication reflects the author's view. The European Union's Horizon 2020 research and innovation programme is not responsible for any use that may be made of the information.

References

[1]Bhandari, P., Birur, G. C., Ganapathi, G., Paris, A. D., Pauken, M., Novak, K., and Tsuyuki, G., "Mechanically Pumped Fluid Loops for Spacecraft Thermal Control: Past, Present & Future," 15th Annual Thermal & Fluid Analysis Workshop, 2004.

[2]van Es, J., Pauw A., van Donk G., Laudi E., Gargiulo C., He Z., Verlaat B., Ragnit U., van Leeuwen P., "AMS02 Tracker Thermal Control Cooling System: Test Results of the AMS02 Thermal Vacuum Test in the LSS at ESA ESTEC", AIAA 2012-3577 (2012)

[3]Lemmon, E.W., Huber, M.L., McLinden, M.O. "NIST Standard Reference Database 23: Reference Fluid Thermodynamic and Transport Properties-REFPROP", Version 9.1, National Institute of Standards and Technology, Standard Reference Data Program, Gaithersburg, 2013

[4]van Gerner, H. J., van Benthem, R. C., van Es, J., Schwaller, D., Lapensée, S., "Fluid selection for space thermal control systems", 44th International Conference on Environmental Systems, ICES-2014-136

[5]van Gerner, H. J., Bolder, R., van Es, J., "Transient modelling of pumped two-phase cooling systems: Comparison between experiment and simulation with R134a", 47th International Conference on Environmental Systems, ICES-2017-037

[6]Incropera, F. P., & DeWitt, *D. P. Fundamentals of heat and mass transfer*. 6th ed. John Wiley & Sons, New York, 2007.

[7]Friedel, L., "Improved friction pressure drop correlation for horizontal and vertical two phase pipe flow," European Two Phase Flow Group Meeting, Ispra, Italy, 1979.

[8]Gungor, K., Winterton, R., "Simplified general correlation for saturated flow boiling and ccomparisons of correlations with data," The Canadian Journal of Chemical Engineering, vol. 65, no. 148, 1987.

[9]Shah, M., "An Improved And Extended general Correlation for Heat Transfer During Condensation in Plain Tubes," HVAC&R Research, vol. 15, pp. 889-913, 2009.

[10]Delcourt, M. O., Belloni, J., Saito, E., "Spectrophotometric studies of the radiolysis of liquid ammonia," The Journal of Physical Chemistry, vol. 80, pp. 1101-1105, 1976.

[11]"German agency seeks ban on R1233zd," 15 8 2017. [Online]. Available: https://www.coolingpost.com/world-news/german-agency-seeks-ban-on-r1233zd/. [Accessed 11 12 2019].

[12]van Gerner, H. J., de Smit, M., van Helvoort, D., van Es, J., "Testing of high heat flux 3D printed aluminium evaporators", 48th International Conference on Environmental Systems, ICES-2018-95

[13]National Fire Protection Association, NFPA 704: "Standard System for the Identification of the Hazards of Materials for Emergency Response"